

# Stepped Impedance Microstrip Directional Coupler With High Directivity Performance

Apisak Worapishet

Mahanakorn Microelectronics Research Centre (MMRC)  
Mahanakorn University of Technology, Nongchok, Bangkok 10530, Thailand  
E-mail: apisak@mut.ac.th

Manuscript received October 17, 2016

Revised December 11, 2016

## ABSTRACT

A directional microstrip coupler utilizing the stepped impedance coupled lines to equalize the even- and odd-mode phase velocities for directivity enhancement is investigated. The stepped impedance coupler features simple analysis, design, and implementation, with small area requirement, no use of lumped reactive components, and no via holes. Experimental results demonstrate a performance improvement in terms of the directivity by as large as 48.6 dB over the conventional coupler.

**Keywords:** Directional coupler, directivity, stepped impedance

## 1. INTRODUCTION

It is known that the conventional microstrip directional coupler suffers from poor directivity. This is primarily attributed to unequal even- and odd-mode phase velocities resulting from the inhomogeneous dielectric of microstrip structures. The directivity performance becomes exacerbated for a coupler with less coupling level and higher permittivity substrate. To enhance the performance, numerous techniques have been introduced to equalize the modal phase velocities. These include the coupler structures using 'wiggly' lines in [1], coupled spurlines in [2], dielectric overlay in [3], re-entrant coupling in [4], and metallic cylinders in [5]. Although these structures are effective in improving the directivity, their designs and optimizations relied heavily on iterative full-wave simulations from the beginning of the design phase. More-over, the structures in [3], [4], [5] are quite complex and require extra processing steps for implementation. Due to its relative simplicity and high directivity, the method of series/ shunt reactive loading, either of capacitive or inductive types [6]–[8], has gained more widespread use. In [8], it is demon-

strated that the coupler structure, which made use of shorted-end stubs through via holes for the shunt inductors, is more suitable for weak coupling levels at high frequencies.

An alternative structure for directivity enhancement in the directional coupler is developed in this paper. In particular, the stepped impedance transmission line technique is incor-porated directly into the coupler structure so as to equalize the modal phase velocities. The stepped impedance coupler offers simple analysis, design and realization. In addition, it occupies small area, and requires no use of lumped reactive components and via holes, which can be difficult to account for at

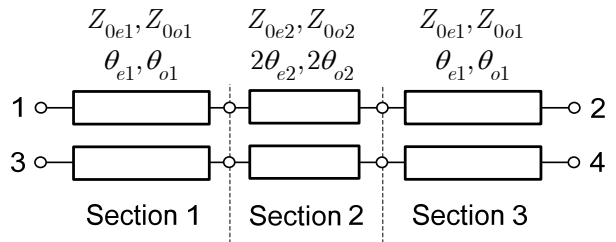


**Fig. 1** Schematic diagram of the stepped impedance coupler.

very high operating frequencies. Detailed analysis is outlined, followed by a design approach. An experimental stepped im-pedance coupler operating at 925 MHz, for use in a domestic UHF RFID system, is provided to verify its practical viability.

## 2. STEPPED IMPEDANCE PARALLEL COUPLER

Fig. 1(a) shows the schematic of the stepped

impedance coupler. It is essentially formed by a cascade of three coupled line sections 1, 2, and 3. Sections 1 and 3 are identical. Their even- and odd-mode characteristic impedances are at  $Z_{0e1}$  and  $Z_{0o1}$ , and the electrical lengths at  $\theta_{e1}$  and  $\theta_{o1}$ , respectively. For section 2, the modal characteristic impedances are at  $Z_{0e2}$  and  $Z_{0o2}$ , and the electrical lengths at  $2\theta_{e2}$  and  $2\theta_{o2}$ . Note that the step impedance ratio in each mode is defined by  $K_{e,o} = Z_{0e1,o1}/Z_{0e2,o2}$ . For a conventional coupler with a uniform coupled line, we have  $K_e = K_o = 1$ .

It is shown in [9] that the first parallel resonance frequency of a stepped impedance transmission line resonator can be *shifted* via adjustment of the stepped impedance ratio. In essence, this indicates that the phase velocity of the wave propagating along the stepped impedance transmission line is modified. Based upon this principle, the incorporation of the stepped impedance structure into coupled microstrip lines to form the stepped impedance couplers enables us to align the even- and odd-mode phase velocities by appropriate selections of the modal stepped impedance ratios  $K_{e,o}$  [10]. As a result, a high directivity microstrip coupler can be achieved.

The stepped impedance coupler can be analyzed by invoking the even- and odd-mode analysis similar to that of the inductive loaded structure in [8]. By applying the even- and odd-mode analysis between port 1 and port 3 of Fig. 1, the coupler is simplified to a set of two identical two-port networks in Fig. 2(a). From these networks, another even- and odd-mode analysis is then applied between port 1 and 2, and between port 3 and 4, with node C as the point of symmetry. This yields the equivalent networks of the resulting four modes as shown in Fig. 2(b)–(e). Since the networks are essentially a cascade of two transmission line sections with open or shorted end, the input impedances of each mode can be derived based on the ABCD matrix of a transmission line section. By setting  $\theta_{e1} = N\theta/\sqrt{\sigma_1}$ ,  $\theta_{o1} = \sigma_1\theta_{e1} = N\theta/\sqrt{\sigma_1}$ ,  $\theta_{e2} = \theta/\sqrt{\sigma_2}$ , and  $\theta_{o2} = \sigma_2\theta_{e2} = \theta\sqrt{\sigma_2}$ , it can be shown that

$$Z_{ee} = -jZ_{01e} \frac{\cos(N\theta/\sqrt{\sigma_1})\cos(\theta/\sqrt{\sigma_2}) - K_o \sin(N\theta/\sqrt{\sigma_1})\sin(\theta/\sqrt{\sigma_2})}{K_e \cos(N\theta/\sqrt{\sigma_1})\sin(\theta/\sqrt{\sigma_2}) + \sin(N\theta/\sqrt{\sigma_1})\cos(\theta/\sqrt{\sigma_2})} \quad (1a)$$

$$Z_{eo} = +jZ_{01e} \frac{\cos(N\theta/\sqrt{\sigma_1})\sin(\theta/\sqrt{\sigma_2}) + K_e \sin(N\theta/\sqrt{\sigma_1})\cos(\theta/\sqrt{\sigma_2})}{K_e \cos(N\theta/\sqrt{\sigma_1})\cos(\theta/\sqrt{\sigma_2}) - \sin(N\theta/\sqrt{\sigma_1})\sin(\theta/\sqrt{\sigma_2})} \quad (1b)$$

$$Z_{oe} = -jZ_{01o} \frac{\cos(N\theta/\sqrt{\sigma_1})\cos(\theta/\sqrt{\sigma_2}) - K_o \sin(N\theta/\sqrt{\sigma_1})\sin(\theta/\sqrt{\sigma_2})}{K_o \cos(N\theta/\sqrt{\sigma_1})\sin(\theta/\sqrt{\sigma_2}) + \sin(N\theta/\sqrt{\sigma_1})\cos(\theta/\sqrt{\sigma_2})} \quad (1c)$$

$$Z_{oo} = +jZ_{01o} \frac{\cos(N\theta/\sqrt{\sigma_1})\sin(\theta/\sqrt{\sigma_2}) + K_o \sin(N\theta/\sqrt{\sigma_1})\cos(\theta/\sqrt{\sigma_2})}{K_o \cos(N\theta/\sqrt{\sigma_1})\cos(\theta/\sqrt{\sigma_2}) - \sin(N\theta/\sqrt{\sigma_1})\sin(\theta/\sqrt{\sigma_2})} \quad (1d)$$

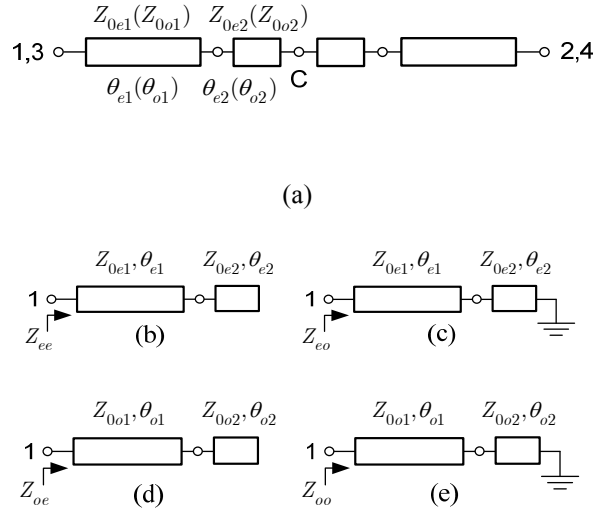


**Fig.2** (a) Even- and Odd-mode equivalent circuits for analysis of the stepped impedance coupler, (b) even mode (ports 1 and 3) followed by even mode (ports 1 and 2), (c) even mode (ports 1 and 3) followed by odd mode (ports 1 and 2), (d) odd mode (ports 1 and 3) followed by even mode (ports 1 and 2), and (e) odd mode (ports 1 and 3) followed by odd mode (ports 1 and 2).

where  $Z_0$  is the system impedance. Note from the equations that, by defining the effective electrical length of a coupled line as  $\theta^{eff} = \sqrt{\theta_e \theta_o}$ , we have  $\theta_1^{eff} = \sqrt{\theta_{e1} \theta_{o1}} = N\theta$  for the coupled line section 1 (and 3), where  $\theta_2^{eff} = \sqrt{\theta_{e2} \theta_{o2}} = \theta$  for the coupled line section 2. Thus,  $N$  represents the ratio between the effective electrical lengths, i.e.,  $N = \theta_1^{eff} / \theta_2^{eff}$ . Also in the equations,  $\sigma_1$  and  $\sigma_2$  are the ratios between the odd- and even-mode electrical lengths for sections 1 (or 3) and section 2, respectively. It is typical that  $\sigma_1 \neq \sigma_2$  because the physical dimensions are different. Under the conditions of an isolation null (or  $S_{41} = 0$ ), and a perfect

match (or  $S_{11} = 0$ ) in the stepped impedance coupler, it was shown in [8] that the following relations must be satisfied:

$$Z_{ee}Z_{oo} = Z_{eo}Z_{oe} \text{ and } Z_0 = \sqrt{Z_{ee}Z_{oo}}. \quad (2)$$

For the coupling parameter  $S_{31}$ , it is given by

$$S_{31} = \frac{1}{2} \left( \frac{(Z_{11e} - Z_0)(Z_{11e} + Z_0) - Z_{21e}^2}{(Z_{11e} + Z_0)^2 - Z_{21e}^2} - \frac{(Z_{11o} - Z_0)(Z_{11o} + Z_0) - Z_{21o}^2}{(Z_{11o} + Z_0)^2 - Z_{21o}^2} \right). \quad (3)$$

As defined in [8],  $Z_{11e} = (Z_{ee} + Z_{eo})/2$ ,  $Z_{11o} = (Z_{oe} + Z_{oo})/2$ ,  $Z_{21e}$

$= (Z_{ee} - Z_{eo})/2$ , and  $Z_{21o} = (Z_{oe} - Z_{oo})/2$ .

The above set of equations (1) to (3) is central to design and optimization of the coupler in order to obtain  $S_{41} = 0$  and  $S_{11} = 0$  at the desired coupling parameter  $|S_{31}|$ . A possible design approach is briefly outlined as follows. Given the parameters of the employed substrate,  $\sigma_{1,2}$  are first approximated from the even- and odd-mode effective dielectric constants,  $\varepsilon_{e,o}^{eff}$ , of the conventional coupled lines at the specified coupling level, where  $\sigma_1 = \sigma_2 = \sqrt{\varepsilon_o^{eff} / \varepsilon_e^{eff}}$ . Next, the ratio  $N$  and the effective electrical length  $\theta$  are selected, and the initial values of the impedances  $Z_{0e1}$  and  $Z_{0o1}$  are assigned. Based upon (1) and (2),  $K_e$  and  $K_o$ , and hence  $Z_{0e2}$  and  $Z_{0o2}$  can be obtained. Since there are no closed form analytical expressions, one must resort to numerical computation. Note that this can be easily executed via manual iterations using a simple mathematical program. The physical dimensions of the stepped impedance coupler are then determined at the operating frequency, and the frequency characteristics are verified via circuit simulation. If the directivity is not satisfied, the design can be refined by recalculating the ratios  $\sigma_{1,2}$ , based on the previously calculated physical dimensions. Subsequently,  $|S_{31}|$  is computed using (3). If not close to the desired value, the variables  $N$ ,  $\theta$ , or  $Z_{0e1}$  and  $Z_{0o1}$  can be adjusted and the ratios  $K_e$  and  $K_o$  recomputed to calculate  $Z_{0e2}$  and  $Z_{0o2}$ . The design flow is iterated until the design converts to the required specifications, and the physical dimensions are realizable under the employed fabrication process. Finally, the design is adjusted and verified using a full-wave simulation, particularly to account for

discontinuities at the layout junctions. It is noted that the above calculation and simulation were executed in this work with the help of a calculation tool, LineCalc, a circuit simulator, ADS, and a full-wave simulator, Momentum, from Agilent [11].

### 3. SIMULATED AND EXPERIMENTAL RESULTS

A stepped impedance microstrip coupler with 12-dB coupling level and 925 MHz operating frequency was designed and fabricated. A Taconic CER-10 substrate, with a high relative dielectric constant of  $\varepsilon_r = 10.0$ , a thickness of 1.57 mm, a 18- $\mu$ m copper cladding, and a loss tangent of 0.0035, was employed.

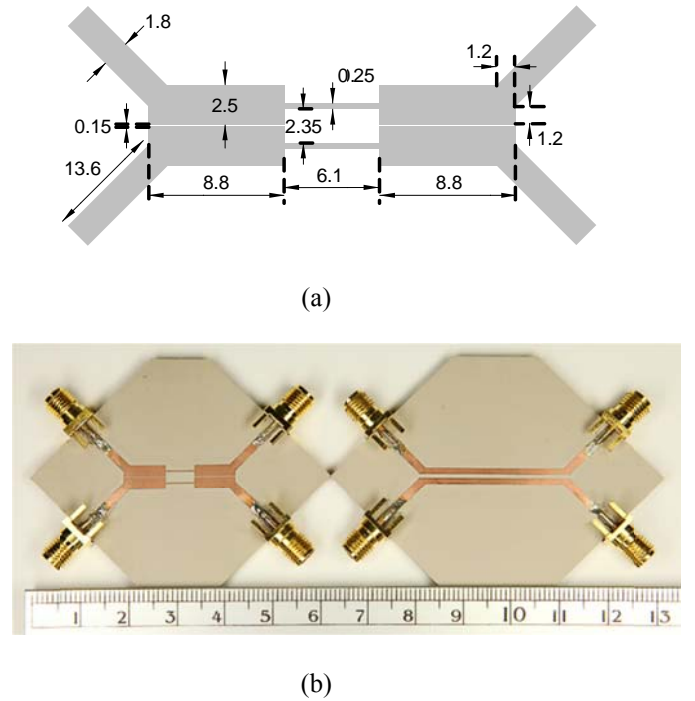


**Fig.3** (a) Final designed dimensions (in mm) and (b) photographs of the stepped impedance coupler and its conventional counterpart.

By following the outlined design methodology, the initial approximations of the modal electrical lengths were  $\sigma_1 = \sigma_2 = 0.886$ . The first design iteration yielded  $N = 3$ ,  $\theta = \pi/16$ ,  $Z_{0e1} = 48 \Omega$ ,  $Z_{0o1} = 22 \Omega$ ,  $Z_{0e2} = 95.90 \Omega$ , and  $Z_{0o2} = 76.44 \Omega$ . After translation to physical dimensions and performing circuit simulation, the simulated directivity was about 26.5 dB at the operating frequency. The variables  $\sigma_{1,2}$  were then recalculated from the physical dimensions of the first design at  $\sigma_1 =$

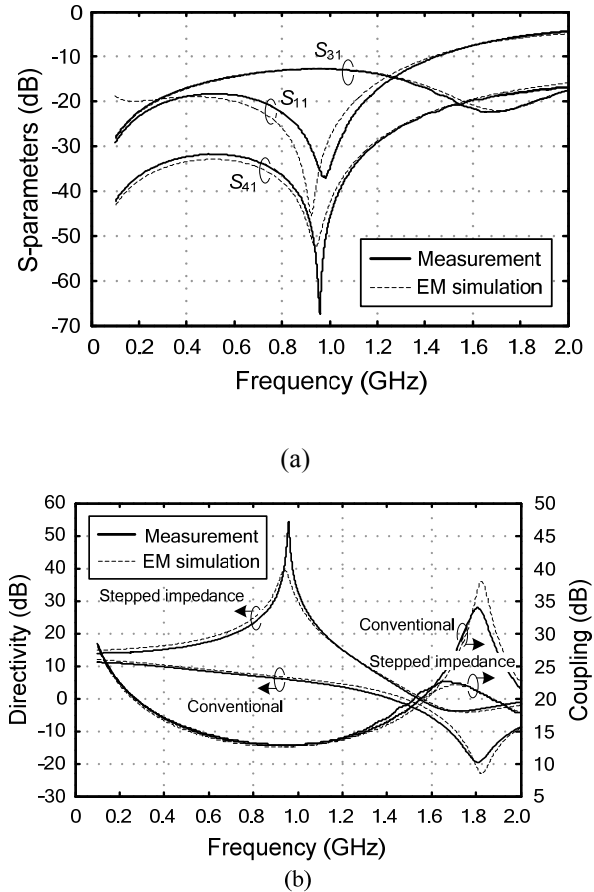
0.855,  $\sigma_2 = 0.922$ . This yielded the modal impedances at  $Z_{0e1} = 48.0 \Omega$ ,  $Z_{0o1} = 22.0 \Omega$ ,  $Z_{0e2} = 92.21 \Omega$ , and  $Z_{0o2} = 72.26 \Omega$ , with the simulated directivity at about 39.8 dB, and the coupling level at 12.8 dB. To obtain the desired coupling level closer to 12 dB, we chose to adjust only the effective electrical length  $\theta$  for simplicity, and repeated the same design flow. The design was completed within five cycles, where  $\sigma_{1,2}$  are finally equal to  $\sigma_1 = 0.855$ ,  $\sigma_2 = 0.926$ , and the designed parameters are as follows:  $N = 3$ ,  $\theta = 0.89 \cdot \pi/16$ ,  $Z_{0e1} = 48.0 \Omega$ ,  $Z_{0o1} = 22.0 \Omega$ ,  $Z_{0e2} = 103.76 \Omega$ , and  $Z_{0o2} = 84.98 \Omega$ , with the directivity of more than 40 dB. After slight adjustments to compensate for the discontinuities at the junctions with the help of a full-wave simulation, the final dimensions of the stepped impedance coupler are as summarized in Fig. 3(a). For the conventional coupler with the same coupling level and operating frequency, the designed parameters are  $Z_{0e} = 63.67 \Omega$  and  $Z_{0o} = 39.26 \Omega$ , with the line's width of  $w = 1.32$  mm, the line spacing  $s$  of 0.83 mm, and the total length of  $l = 31.9$  mm.

Fig. 3(b) shows the photographs of the stepped impedance coupler and the conventional counterpart. The measurement was performed using an Agilent N5230A Vector Network Analyzer with the Short-Open-Load-Through (SOLT) calibration module. The measured  $S$ -parameters of the stepped impedance coupler are given in Fig. 4(a) where it can be deduced that the coupling and isolation levels at 925 MHz are at 12.78 dB and 48.9 dB, respectively. The return loss is more than 30.8 dB. Also, the maximum isolation at 959 MHz. As indicated by the figure, the measurement is in good agreement with simulation. Fig. 4(b) shows the simulated and measured responses of the directivities and coupling levels for both the couplers. It can be seen that the stepped impedance structure exhibits a higher directivity by more than 30 dB at the operating frequency, and the maximum improvement can be as large as 48.6 dB.

#### 4. CONCLUSION

The directional coupler structure which relies upon the use of the stepped impedance coupled lines for high directivity has been developed. The coupler has been analyzed, and a simple design approach has been provided, which is mainly based on the derived equations with intervention of full-wave simulation only at the final design phase. Demonstration was given via an experimental designed coupler, where a maximum improvement of more than 48.6 dB in the directivity

performance over the conventional counterpart was achieved.



**Fig.4** (a) Simulated and measured frequency responses, and (b) comparisons of directivities and coupling levels.

#### REFERENCES

- [1] A. Podell, "A high directivity microstrip coupler technique," in *IEEE MTT-S Int. Microw. Symp. Dig.*, May 1970, pp. 33–36.
- [2] S.-F. Chang, J.-L. Chen, Y.-H. Jeng, and C.-T. Wu, "New high-directivity coupler design with coupled spurlines," *IEEE Microw. Wireless Compon. Lett.*, vol. 14, no. 2, pp. 65–67, Feb. 2004.
- [3] L. Su, T. Itoh, and J. Rivera, "Design of an overlay directional coupler by a full-wave analysis," in *IEEE MTT-S Int. Microw. Symp. Dig.*, May 1983, pp. 427–429.
- [4] C.-S. Kim, S.-W. Lee, P.-Y. Lee, H.-S. Kim, J.-S. Park, and D. Ahn, "Design of re-entrant mode microstrip directional coupler for high directivity performance," *Asia-Pacific, Microwave Conf.*, 2000, pp. 1286–1289.
- [5] J. Shi, X.Y. Zhang, K.W. Lau, J.-X. Chen, and Q. Xue, "Directional coupler with high directivity using metallic cylinders on microstrip line" *Electron. Lett.*, vol. 45, no. 8, pp. 415–417, Apr. 2009.
- [6] M. Dydyk, "Microstrip directional couplers with ideal performance via single-element compensation," *IEEE Trans. Microw. Theory Tech.*, vol. 47, no. 6, pp. 956–964, Jun. 1999.

- [7] R. Phromloungsri, M. Chongcheawchamnan, and I. D. Robertson, "Inductively compensated parallel coupled microstrip lines and their applications," *IEEE Trans. Microw. Theory Tech.*, vol. 54, no. 9, pp.3571–3582, Sep. 2006.
- [8] S. Lee, and Y. Lee, "A design method for microstrip directional couplers loaded with shunt inductors for directivity enhancement," *IEEE Trans. Microw. Theory Tech.*, vol. 58, no. 4, pp. 994–1002, Apr. 2010.
- [9] M. Makimoto and S. Yamashita, "Bandpass filters using parallel coupled stripline stepped impedance resonators," *IEEE Trans. Microw. Theory Tech.*, vol. MTT-28, no. 12, pp. 1413-1417, Dec. 1980.
- [10] A. Worapishet, S. Srisathit, W. Surakumpontorn, "Stepped-Impedance coupled resonators for implementation of parallel coupled microstrip filters with spurious band suppression," *IEEE Trans. Microw. Theory Tech.*, vol. MTT-60, no. 6, pp. 1540-1548, Jun. 2012.
- [11] Advanced Design System (ADS) 2009. Agilent Technol., Palo Alto, CA, 2009. (<http://www.agilent.com/find/eesof-ads>)



**Apisak Worapishet** received the B.Eng. degree (with first-class honors) from King Mongkut's Institute of Technology Ladkrabang, Bangkok, Thailand, in 1990, the M.Eng.Sc. degree from the University of New South Wales, Australia, in 1995, and the Ph.D. degree from Imperial College, London, U.K., in 2000, all in electrical engineering. Since 1990, he has been with Mahanakorn University of Technology, Bangkok, Thailand, where he currently serves as the Director of Mahanakorn Microelectronics Research Center (MMRC). He also serves as the Editor-In-Chief of the ECTI Transactions on EEC, and the Associate Editor of IEEE Transactions on Circuits and Systems – I, Regular Papers. His current research interest includes mixed-signal CMOS analog integrated circuits, Bio-medical sensors, wirelined and wireless RF CMOS circuits, microwave circuits, reconfigurable and embedded circuits and systems.